Journal of Inclusion Phenomena and Macrocyclic Chemistry (2006) 55:359–366
DOI 10.1007/s10847-006-9108-z

Organotins as a Locking Agent in the Formation of Dinuclear Complexes

K.S. SIDDIQI*, SADAF KHAN and SHAHAB A.A. NAMI
Department of Chemistry, Aligarh Muslim University, 202002, Aligarh, India

(Received: 19 October 2005; in final form: 1 March 2006)

Key words: heterobimetallic compounds, locking agent, TGA/DSC

Abstract

In this paper the synthesis and characterization of new heterobimetallic compounds with a ligand derived from diacetylpyridine, hydrazine and salicylaldehyde has been reported. The open end of the ligand was locked with R_2SnCl_2 followed by the insertion of a transition metal ion in the cavity thus formed by locking the ligand. These compounds are characterized by TGA/DSC, IR, ^1H and ^{13}CNMR, electronic spectra, magnetic moment and conductivity measurements. The disappearance of ν(O–H) and appearance of ν(Sn–O) in the IR spectrum of the Sn(saldp)R_2 {where saldp = bis(salicylaldehydehydrazone)diacetylpyridine and R = $-CH_3$, $-C_4H_9$} suggests the complex formation with R_2SnCl_2. The IR spectra of the complexes exhibited a blue shift in ν(C=N) indicating coordination of the azomethine nitrogen. The complexes are non-electrolytes in DMSO. The ^1HNMR and ^{13}CNMR spectra of the complexes are not much different from that of the free ligand except for the disappearance of the signal at 9 ppm due to phenolic protons. The methyl or butyl protons attached to the tin appear at their usual places. The TGA profile of the ligand and its mononuclear complexes exhibit a three-step pyrolysis, although the binuclear complexes decompose in two steps leaving behind tin oxide as the final product.

Introduction

Compartmental ligands, their mononuclear and dinuclear complexes have attracted a lot of attention in the recent years due to the key role they play in many synthetic and biological applications. Dinuclear metal complexes have been successfully used for the recognition and assembly of various organic and inorganic moieties [1–3]. They are also employed as models for active centers of various metalloenzymes such as tyrosine which effects skin pigmentation [4] and as successful devices, to host and carry small molecules or ions as a guest and as catalyst [5]. Consequently, several workers have continued to investigate the structural and magneto chemical aspects of binuclear complexes with a variety of bridging systems [6–7]. Since heterodinuclear complexes containing both transition as well as non transition metal ions are scarce [8], we are attempting, to probe the structural, magneto-chemical and thermal properties of heterodinuclear complexes containing late 3-d transition metal ions and dialkyltindihalides. In continuation of our work on dinuclear systems [9–10], we are reporting, a novel compartmental ligand composed of diacetylpyridine, hydrazine and salicylaldehyde, H_2saldp (where saldp = bis(salicylaldehydehydrazone)diacetylpyridine). Although, diorganotins [R_2SnX_2] have been studied extensively as anticancer agents their use as ring closing agents is limited [11]. In the present study, diorganotin dichlorides R_2SnCl_2 (R = Me, Bu) have been exploited as locking agents leading to the formation of a cavity of appropriate size [12] that encapsulates a transition metal ion.

Experimental

Hydrated metal chlorides (BDH), salicylaldehyde, diacetylpyridine (Fluka) and hydrazine hydrate (Ranbaxy) were used as received. Methanol was used after distillation. Elemental analyses were carried out with a Perkin Elmer, Series II CHNS/O analyzer 2400, USA. Chloride was determined gravimetrically as AgCl [13]. IR spectra (4000–200 cm^{-1}) were recorded on a RXI FT-IR spectrometer as KBr discs. The conductivity measurements were carried out with CM-82T Elico conductivity bridge in DMSO. The electronic spectra were recorded on a Cintra 5GBC spectrophotometer in DMSO. Magnetic susceptibility measurements were done with a 155 Allied Research vibrating sample magnetometer at room temperature. The NMR spectra were recorded on a DPX-300 spectrometer in DMSO at room temperature. ^{13}CNMR spectra were recorded in $CDCl_3$. The TGA was performed with a Perkin Elmer thermal analyzer under nitrogen atmosphere

* Author for Correspondence. E-mail: khwajas_siddiqi@yahoo.co.in

using calcinated Al_2O_3 as reference. The weight of the sample taken was 8 mg. The heating rate was kept at 10 °C min^{-1}. Melting points were determined by the Wiswo melting point apparatus. The metal contents were estimated by complexometric titrations [14].

Preparation of H_2saldp

Hydrazine hydrate (10 mmol, 0.5 mL) was dropwise added to a solution of 2,6-diacetylpyridine (5 mmol, 0.82 g) dissolved in 25 mL of acetonitrile. After 2 h of stirring, a white precipitate was obtained which was left overnight. It was decanted, washed several times with acetonitrile and cold diethylether and dried *in vacuo* over $CaCl_2$. The methanolic solution (25 mL) of this white precipitate (2 mmol, 0.38 g) was, subsequently allowed to react with salicylaldehyde (4 mmol, 0.42 mL). A yellow precipitate thus obtained was decanted, washed several times with methanol and ether and dried *in vacuo* (Figure 1). Anal. Calcd. for H_2saldp, $C_{23}H_{21}N_5O_2$: C, 69.2; H, 5.3; N, 17.5. Found: C, 69.0; H, 5.2; N, 17.4. m.p. 109 °C, Yield, 55%.

Preparation of mononuclear complexes, Sn(saldp)R_2

To a methanolic solution 25 mL of H_2saldp (2 mmol, 0.38 gm), R_2SnCl_2 (where R = CH_3 and C_4H_9) (2 mmol) dissolved in 20 mL of the same solvent was added, dropwise with continuous stirring. The reaction mixture was stirred for about 2 h to obtain a light-yellow thick precipitate. It was filtered through celite washed with methanol, cold diethyl ether and dried *in vacuo* (Figure 2). Anal. Calcd. for $[(C_{23}H_{19}N_5O_2)Sn(CH_3)_2]$: C, 54.9; H, 4.6; N, 12.8; Sn, 21.7. Found: C, 54.8; H, 4.5; N, 12.7; Sn, 21.6. m.p. 144 °C, Yield, 62%. Calcd. for $[(C_{23}H_{19}N_5O_2)Sn(C_4H_9)_2]$: C, 59.0; H, 5.9; N, 11.1; Sn, 18.8. Found: C, 58.9; H, 5.8; N, 11.0; Sn, 18.7. m.p. 191 °C, Yield, 67%.

Preparation of heterodinuclear complexes, Sn(saldp)R_2MX_2

In a well dissolved 20 mL methanolic solution of Sn(saldp)R_2 (2 mmol), hydrated metal chloride (2 mmol) dissolved in the same solvent (20 mL) was added, dropwise to obtain an immediate precipitation of the respective binuclear complexes. The precipitate was decanted washed with methanol and cold diethyl ether and dried *in vacuo* (Figure 3).

Anal. Calcd. for $[(C_{23}H_{19}N_5O_2)Sn(CH_3)_2MnCl_2]$: C, 44.7; H, 3.8; N, 10.4; Sn, 17.7: Mn, 8.2.
Found: C, 44.5; H, 3.7; N, 10.4; Sn, 17.5: Mn, 8.3. m.p. 183 °C, Yield, 70%.
Calcd. for $[(C_{23}H_{19}N_5O_2)Sn(CH_3)_2FeCl_2]$: C, 44.6; H, 3.7; N, 10.4; Sn, 17.6: Fe, 8.3.

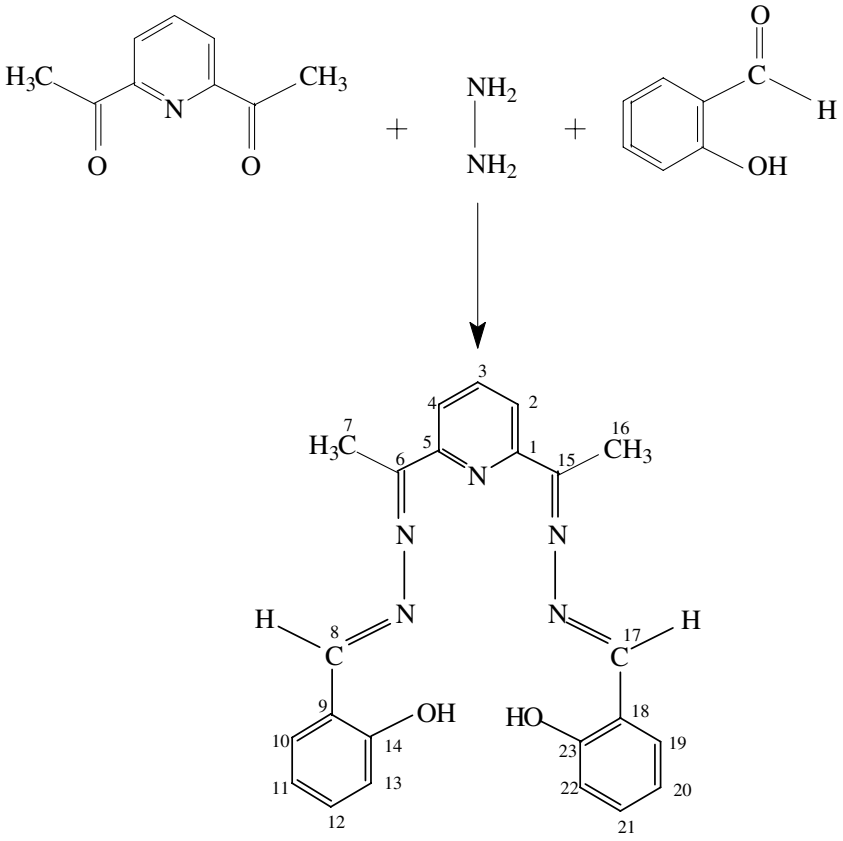

Figure 1. Preparation of H_2saldp.

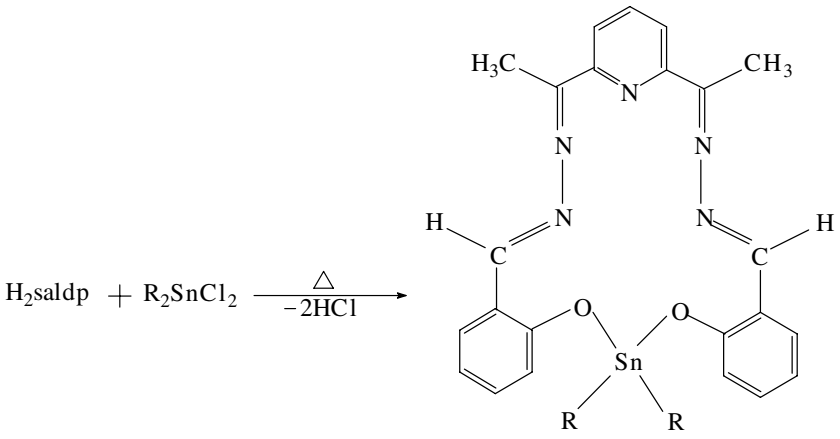

Figure 2. Preparation of mononuclear Sn(saldp)R_2.

Found: C, 44.4; H, 3.6; N, 10.4; Sn, 17.5: Fe, 8.4. m.p. 103 °C, Yield, 68%.

Calcd. for $[(C_{23}H_{19}N_5O_2)Sn(CH_3)_2CoCl_2]$: C, 44.4; H, 3.7; N, 10.4; Sn, 17.5: Co, 8.7.

Found: C, 44.3; H, 3.6; N, 10.3; Sn, 17.0: Co, 8.8. m.p. 171 °C, Yield, 55%.

Calcd. for $[(C_{23}H_{19}N_5O_2)Sn(CH_3)_2NiCl_2]$: C, 44.4; H, 3.7; N, 10.4; Sn, 17.6; Ni, 8.7.

Found: C, 44.2; H, 3.4; N, 10.3; Sn, 17.4: Ni, 8.9. m.p. 118 °C, Yield, 48%.

Calcd. for $[(C_{23}H_{19}N_5O_2)Sn(CH_3)_2CuCl_2]$: C, 44.1; H, 3.7; N, 10.3; Sn, 17.4: Cu, 9.3.

Found: C, 44.0; H, 3.6; N, 10.2; Sn, 17.3: Cu, 9.4. m.p. 149 °C, Yield, 72%.

Anal. Calcd. for $[(C_{23}H_{19}N_5O_2)Sn(C_4H_9)_2MnCl_2]$: C, 49.2; H, 4.9; N, 9.3; Sn, 15.7: Mn, 7.3.

Found: C, 49.0; H, 4.8; N, 9.2; Sn, 15.6: Mn, 7.4. m.p. 160 °C, Yield, 70%.

Calcd. for $[(C_{23}H_{19}N_5O_2)Sn(C_4H_9)_2FeCl_2]$: C, 49.2; H, 4.9; N, 9.2; Sn, 15.7: Fe, 7.4.

Found: C, 49.0; H, 4.4; N, 9.2; Sn, 15.4: Fe, 7.5. m.p. 130 °C, Yield, 70%.

Calcd. for $[(C_{23}H_{19}N_5O_2)Sn(C_4H_9)_2CoCl_2]$: C, 48.9; H, 4.9; N, 9.2; Sn, 15.6: Co, 7.7.

Found: C, 48.8; H, 4.6; N, 9.1; Sn, 15.2: Co, 7.9. m.p. 185 °C, Yield, 65%.

Calcd. for $[(C_{23}H_{19}N_5O_2)Sn(C_4H_9)_2NiCl_2]$: C, 48.9; H, 4.9; N, 9.2; Sn, 15.6; Ni, 7.7.

Found: C, 48.3; H, 4.8; N, 9.2; Sn, 15.0: Ni, 7.8. m.p. 135 °C, Yield, 58%.

Calcd. for $[(C_{23}H_{19}N_5O_2)Sn(C_4H_9)_2CuCl_2]$: C, 48.7; H, 4.9; N, 9.1; Sn, 15.5: Cu, 8.3.

Found: C, 48.4; H, 4.6; N, 9.1; Sn, 15.2: Cu, 8.4. m.p. 155 °C, Yield, 60%.

Results and discussion

The mononuclear complexes are conveniently obtained by the facile reaction between H_2saldp and R_2SnCl_2 (Figures 2 and 3) in 1:1 stoichiometry.

$$H_2\text{saldp} + R_2SnCl_2 \rightarrow Sn(\text{saldp})R_2 + 2HCl$$

However,the binuclear complexes are obtained by simple insertion reaction of transition metal halides in the cavity formed by Sn(saldp)R_2 in alcoholic medium. Their molar conductance of 1 mM solutions measured

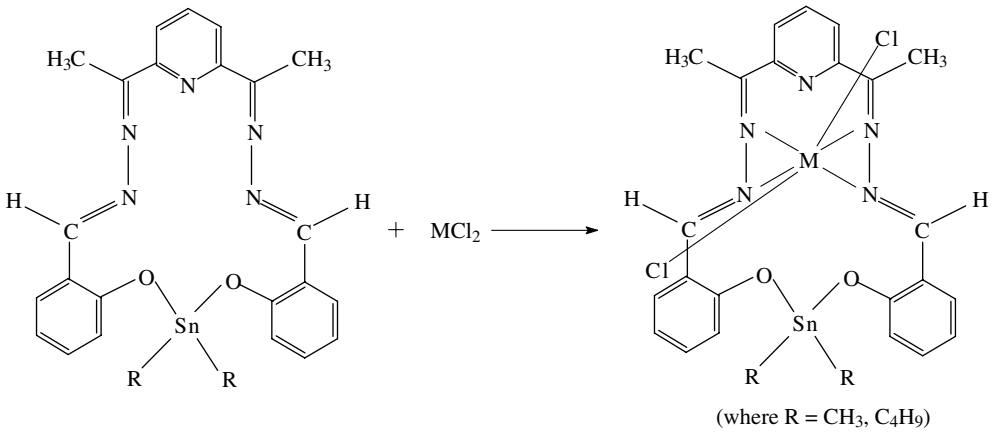

Figure 3. Preparation of binuclear complexes.

in DMSO indicated that they are non-electrolytes [15]. The complexes are stable to heat and light. They are amorphous in nature, partially soluble in $CHCl_3$, CH_2Cl_2 and highly soluble in DMSO and DMF. An attempt is being made to recrystallize them in order to get their crystal structure solved.

IR spectra

The diagnostic IR bands of the complexes are summarized in Table 1. The ligand and its mononuclear complexes exhibit an intense band in 1648–1630 cm^{-1} range due to azomethine nitrogen (C = N) [16]. It indicates the condensation of the C = O groups of salicylaldehyde with the amino groups of the flanked hydrazine moiety, affording the ligand H_2saldp. However, in the binuclear complexes ν(C = N) is shifted to a lower region (Figure 3) indicating coordination of the metal ions with the azomethine nitrogen [17]. A medium intensity band at 3356 cm^{-1}, characteristic of ν(O–H) of the ligand was found to be absent in the complexes (Figure 2).

The far-IR region is quite cardinal in the present study. In all the metal complexes the presence of a medium intensity band in 255–298 cm^{-1} range assignable to ν(Sn–O) [18], establishes the use of R_2SnCl_2 as a locking agent and the formation of a cavity. As there is only one band in this region a linear O–Sn–O coordination is expected [19]. The medium intensity bands observed at 1450 and 1357 cm^{-1} can be associated with the composite ν(C = C) and ν(C = N) vibrations in agreement with the other authors [20].

Occurrence of some new bands in the far-IR range (330–380 cm^{-1}) is consistent with the ν(M–N) [21].

Electronic spectra and magnetic moments

The electronic spectral bands and the magnetic moments of the complexes are summarized in Table 2. An octahedral Mn(II) complex gives spin forbidden as well as parity-forbidden bands [22]. In addition to the band due to n–π^* transition the electronic spectrum of Mn(II) complex in DMSO exhibits three spectral bands in the region 31,521–30,735 cm^{-1}; 23,454–21,453 cm^{-1} and 17,851–17,689 cm^{-1} which have been assigned to $^4T_1g(P) \leftarrow {}^6A_{1g}$; $^4T_2g(G) \leftarrow {}^6A_{1g}$ and $^4T_1g(G) \leftarrow {}^6A_{1g}$ transitions, respectively. The high spin d^5 configuration gives an essentially spin-only magnetic moment of ~5.9 B.M. and is temperature independent. The magnetic moment in this case is very close to spin free octahedral Mn(II) ion [23].

The room temperature magnetic moment values are found to be 5.09 and 5.21 B.M. for Sn(saldp)Me_2FeCl_2 and Sn(saldp)$BuFeCl_2$ complexes, respectively. These values are in close agreement with those of Fe(salen) [24] and Fe(salen)py_2 [25]. The electronic spectrum of Fe(II) complexes display two charge transfer bands besides a broad d–d band (Table 2). The charge transfer bands observed in the 28,000–33,400 cm^{-1} might be due to π–π^* transition [26] of the azomethine group.

The spectra of Sn(saldp)Me_2CoCl_2 and Sn(saldp)-Bu_2CoCl_2 have identical features, indicating similar stereochemistry around the Co(II) ion. The former shows absorptions at 20,790, 15,552 and 11,146 cm^{-1} and the latter exhibits bands at 22,321, 16,474 and 11,272 cm^{-1} (Table 2). The low frequency band at around 11,000 cm^{-1} is characteristic of Co(II) ion with an octahedral arrangement [27]. The observed magnetic moment values (4.14 and 4.20 B.M.) are within the predicted range for a high-spin Co(II) ion with considerable orbital contribution to the overall magnetic moment [28].

Electronic spectra of octahedral Ni(II) complex is known to exhibit three spin allowed electronic transitions from $^3A_{2g}$ ground state to $^3T_{1g}(P)$, $^3T_{1g}(F)$ and $^3T_{2g}(F)$ excited states, respectively [29]. In the case of Sn(saldp)Me_2NiCl_2 and Sn(saldp)Bu_2NiCl_2, three absorption bands in the range 22,779–22,371 cm^{-1} (ν_1), 15,847–15,384 cm^{-1} (ν_2) and 11,764–12,544 cm^{-1} (ν_3) have been observed. The ν_1 due to one of the spin allowed electronic transitions in the visible region is

Table 1. Diagnostic IR bands of ligand and its monometallic and bimetallic analogs

Complex	ν(O–H)	ν(C = N)	Composite		ν(M–N)	ν(M–Cl)	ν(Sn–O)
			ν(C = C)	ν(C = N)			
H_2saldp	3356 s	1638 s	1450 m	1357 m	–	–	–
Sn(saldp)Me_2	–	1620 s	1450 m	1357 m	478 m	–	293 m
Sn(saldp)Bu_2	–	1620 s	1450 m	1357 m	424 m	–	293 m
Sn(saldp)Me_2MnCl_2	–	1620 s	1450 m	1357 m	432 m	354 m	300 m
Sn(saldp)Me_2FeCl_2	–	1620 s	1450 m	1357 m	438 m	347 m	255 m
Sn(saldp)Me_2CoCl_2	–	1620 s	1450 m	1357 m	424 m	362 m	278 m
Sn(saldp)Me_2NiCl_2	–	1620 s	1450 m	1357 m	416 s	331 m	287 m
Sn(saldp)Me_2CuCl_2	–	1620 s	1450 m	1357 m	432 m	339 m	298 m
Sn(saldp)Bu_2MnCl_2		1620 s	1450 m	1357 m	432 m	324 m	285 m
Sn(saldp)Bu_2FeCl_2	–	1620 s	1450 m	1357 m	416 m	301 m	293 m
Sn(saldp)Bu_2CoCl_2	–	1620 s	1450 m	1357 m	486 m	331 m	268 m
Sn(saldp)Bu_2NiCl_2	–	1620 s	1450 m	1357 m	478 m	308 m	278 m
Sn(saldp)Bu_2CuCl_2	–	1620 s	1450 m	1357 m	424 m	362 m	276 m

Table 2. Magnetic susceptibility, electronic spectra and ligand field parameters of the complexes

Compounds	Magnetic moment (B.M.)	Electronic bands (cm^{-1})	Log ϵ (mol^{-1} cm^2)	Possible assignments	10 Dq (cm^{-1})	B (cm^{-1})	β
$Sn(saldp)Me_2MnCl_2$	5.78	30,735	2.9	$^4T_{1g}(P) \leftarrow {}^6A_{1g}$	17,670	427	0.83
		21,453	2.4	$^4T_{2g}(G) \leftarrow {}^6A_{1g}$			
		17,689	2.0	$^4T_{1g}(G) \leftarrow {}^6A_{1g}$			
$Sn(saldp)Me_2FeCl_2$	5.30	16,572	3.2	$^5E_g \leftarrow {}^5T_{2g}$	16,572	–	–
$Sn(saldp)Me_2CoCl_2$	4.14	20,790	2.7	$^4T_{1g}(P) \leftarrow {}^4T_{1g}(F)$	12,030	334	0.65
		15,552	2.5	$^4A_{2g}(F) \leftarrow {}^4T_{1g}(F)$			
		11,146	2.2	$^4T_{2g}(F) \leftarrow {}^4T_{1g}(F)$			
$Sn(saldp)Me_2NiCl_2$	3.21	22,371	2.6	$^3T_{1g}(P) \leftarrow {}^3A_{2g}(F)$	11,760	392	0.62
		15,847	2.2	$^3T_{1g}(F) \leftarrow {}^3A_{2g}(F)$			
		11,764	1.8	$^3T_{2g}(F) \leftarrow {}^3A_{2g}(F)$			
$Sn(saldp)Me_2CuCl_2$	1.91	21,005	2.7	$^2E_g \leftarrow {}^2B_{1g}$	–	–	–
$Sn(saldp)Bu_2MnCl_2$	5.81	31,521	2.9	$^4T_{1g}(P) \leftarrow {}^6A_{1g}$	16,785	439	
		23,454	2.3	$^4T_{2g}(G) \leftarrow {}^6A_{1g}$			
		17,851	2.0	$^4T_{1g}(G) \leftarrow {}^6A_{1g}$			
$Sn(saldp)Bu_2FeCl_2$	5.44	16,475	2.9	$^5E_g \leftarrow {}^5T_{2g}$	16,475	–	0.85
$Sn(saldp)Bu_2CoCl_2$	4.20	22,321	2.5	$^4T_{1g}(P) \leftarrow {}^4T_{1g}(F)$	12,080	402	–
		16,474	2.4	$^4A_{2g}(F) \leftarrow {}^4T_{1g}(F)$			
		11,272	2.5	$^4T_{2g}(F) \leftarrow {}^4T_{1g}(F)$			
$Sn(saldp)Bu_2NiCl_2$	3.34	22,779	2.4	$^3T_{1g}(P) \leftarrow {}^3A_{2g}(F)$	12,380	279	0.78
		15,384	1.7	$^3T_{1g}(F) \leftarrow {}^3A_{2g}(F)$			
		12,544	1.4	$^3T_{2g}(F) \leftarrow {}^3A_{2g}(F)$			
$Sn(saldp)Bu_2CuCl_2$	1.94	19,608	2.6	$^2E_g \leftarrow {}^2B_{1g}$	–	–	–

assigned to $^3T_{1g}(P) \leftarrow {}^3A_{2g}(F)$. The position of middle band (ν_2) has been attributed to $^3T_{1g}(F) \leftarrow {}^3A_{2g}$ transition. The ligand field parameters viz. 10 Dq, B (Racah parameter), β (Nephelauxetic ratio) are almost identical for $Sn(saldp)Me_2NiCl_2$ and $Sn(saldp)Bu_2NiCl_2$. These values reflect that the M–L bond is sufficiently strong, which in turn suggests enough overlapping of metal orbitals with those of the ligand. The compounds are paramagnetic with room temperature magnetic moment values ranging between 3.21 and 3.34 B.M.

Octahedral Cu(II) complexes are known to exhibit four absorption bands, but only one broad band is generally observed [30]. Such a case arises due to the masking of less intense d–d bands by the strong charge transfer bands [31]. In the present study a broad band in 21,005–19,608 cm^{-1} (Table 2) has been observed. Practically, for an octahedral Cu(II) complex the room temperature magnetic moment value ranges between 1.8 and 2.0 B.M. [32]. In the present work, the small increase from the spin-only value is due to the mixing of some orbital angular momentum from excited states via spin–orbit coupling phenomenon [33]. The electronic spectra and the magnetic moment data are consistent with an octahedral structure for Cu(II) ion.

TGA/DTG

The samples were heated at uniform rate of 20 °C min^{-1}. The TGA profile of the ligand (H_2saldp) consists of two well-defined stages (Table 3). The first decomposition stage starts at 110 °C and continues [34] until 470 °C. It corresponds to the degradation of two salicylaldehyde moieties contributing 57.14% weight loss (calcd. 57.15%). The second stage starts from 500 °C and continues until 800 °C which is consistent with the degradation of the remaining part of the molecule. Generally, the TGA steps corresponding to deamination involve sudden weight losses, accompanied by relatively sharp peaks in corresponding DTG curve [35].

In the present case, the DTG curve of the ligand shows an intense sharp exothermic peak for the rapid pyrolysis of salicylaldehyde moieties. However, there is no distinct peak corresponding to the second step.

The mononuclear complexes exhibit three stage thermograms in the range 200–350, 350–450 and 450–800 °C, respectively. The first stage accounts for about 20% weight loss corresponding to the degradation of diacetylpyridine fragment while the second stage corresponds to the liberation of two nitrogen molecules. The third stage of pyrolysis is consistent with the decomposition of the remaining part of the molecule containing Sn as SnO_2 [36]. The DTG profile in the present case is quite diagnostic. A sharp exothermic peak is observed for the first step while a weak endotherm may be attributed to the liberation of nitrogen. Moreover, a sharp exothermic peak in the end corresponds to the oxidation of Sn to SnO_2.

The TGA profile of the bimetallic complexes is relatively simple and consists of two discrete stages. The initial stage corresponds to the simultaneous loss of chlorine, diacetylpyridine and two alkyl groups. The

Table 3. Thermal degradation of various fragments of ligand and its complexes

Complexes	First decomposition stage			Second decomposition stage			Third decomposition stage		
	Fragments	Temp. range (°C)	Mass loss data, found (calcd.) %	Fragments	Temp. range (°C)	Mass loss data, found (calcd.) %	Fragments	Temp. range (°C)	Mass loss data, found (calcd.) %
H_2saldp	Two salicylaldehyde moieties	50–471	57.14 (57.15)	Remaining organic moiety	472–500	42.68 (42.85)	–	–	–
Sn(saldp)Me_2	Diacetyl pyridine	100–273	19.14 (19.05)	Two methyl groups + two nitrogen molecules	274–322	16.04 (16.01)	Remaining organic moiety + SnO_2	323–450	64.69 (64.94)
Sn(saldp)Bu_2	-do-	100–472	17.38 (17.12)	Two butyl groups + two nitrogen molecules	470	68.41 (68.68)	-do-	550–700	23.06 (23.12)
Sn(saldp)Me_2MnCl_2	-do-	150–192	16.12 (16.01)	-do-	200–550	13.48 (13.37)	Remaining organic moiety including Mn + SnO_2	550–700	70.27 (70.62)
Sn(saldp)Me_2FeCl_2	-do-	147–194	16.05 (15.99)	-do-	200–550	13.46 (13.35)	Remaining organic moiety including Fe + SnO_2	550–700	70.27 (70.66)
Sn(saldp)Me_2CoCl_2	-do-	145–190	16.03 (15.91)	-do-	200–550	13.38 (13.28)	Remaining organic moiety including Co + SnO_2	550–700	70.59 (70.81)
Sn(saldp)Me_2NiCl_2	-do-	147–194	15.99 (15.92)	-do-	200–550	13.38 (13.29)	Remaining organic moiety including Ni + SnO_2	550–700	70.59 (70.79)
Sn(saldp)Me_2CuCl_2	-do-	145–189	15.89 (15.80)	-do-	200–550	13.26 (13.19)	Remaining organic moiety including Cu + SnO_2	550–700	70.89 (71.01)
Sn(saldp)Bu_2MnCl_2	-do-	210–428	14.16 (14.10)	-do-	439–636	23.38 (23.20)	Remaining organic moiety including Mn + SnO_2	637–700	62.46 (61.93)
Sn(saldp)Bu_2FeCl_2	-do-	100–306	14.14 (14.09)	-do-	307–400	23.35 (23.29)	Remaining organic moiety including Fe + SnO_2	401–500	62.51 (62.11)
Sn(saldp)Bu_2CoCl_2	-do-	100–300	14.08 (14.00)	-do-	300–410	23.25 (23.12)	Remaining organic moiety including Co + SnO_2	411–600	62.67 (62.30)
Sn(saldp)Bu_2NiCl_2	-do-	100–200	14.09 (13.99)	-do-	201–375	23.26 (23.00)	Remaining organic moiety including Ni + SnO_2	376–600	62.65 (62.42)
Sn(saldp)Bu_2CuCl_2	-do-	100–250	13.99 (13.87)	-do-	251–450	23.11 (23.01)	Remaining organic moiety including Cu + SnO_2	452–600	62.90 (62.78)

Table 4. ^{1}H NMR spectra of the ligand and its complexes

Complex	$\delta(CH_3)$ of diacetylpyridine	δ(C–H) of salicylaldehyde	δ(O–H) of salicylaldehyde
H_2saldp	2.18 (s)	6.99 (s)	9.0 (s)
Sn(saldp)Me_2	2.15 (s)	6.99 (s)	–
Sn(saldp)Bu_2	2.17 (s)	6.99 (s)	–
Sn(saldp)Me_2MnCl_2	2.18 (s)	6.99 (s)	–
Sn(saldp)Me_2FeCl_2	2.19 (s)	6.99 (s)	–
Sn(saldp)Me_2CoCl_2	2.19 (s)	6.98 (s)	–
Sn(saldp)Me_2NiCl_2	2.14 (s)	6.99 (s)	–
Sn(saldp)Me_2CuCl_2	2.17 (s)	6.99 (s)	–
Sn(saldp)Bu_2MnCl_2	2.20 (s)	6.98 (s)	–
Sn(saldp)Bu_2FeCl_2	2.18 (s)	6.97 (s)	–
Sn(saldp)Bu_2CoCl_2	2.20 (s)	6.98 (s)	–
Sn(saldp)Bu_2NiCl_2	2.20 (s)	6.98 (s)	–
Sn(saldp)Bu_2CuCl_2	2.21 (s)	6.97 (s)	–

Note: ^{1}H NMR of (C_5H_5N) and (C_6H_5) appear as a multiplet in the range $\delta = 8.2$–8.8 and 7.4–7.6 respectively.

second stage corresponds to the degradation of the remaining part of the molecule containing Sn in its oxide form. The DTG curve exhibits a solitary peak in the 200–350 °C range.

^{1}HNMR and ^{13}CNMR spectra

The ^{1}HNMR spectra of the H_2saldp exhibits singlets at δ = 2.18 and 6.99 ppm corresponding to the methyl protons of the diacetyl moiety and C–H of the salicylaldimine moiety, respectively [37]. Two sets of multiplets were observed at δ = 8.2–8.8 due to the pyridinium protons while the multiplet at δ = 7.4–7.6 corresponds to the phenyl protons of the salicylaldimine moiety [38] of the ligand and its complexes (Table 4). A low field signal at δ = 9.0 ppm may be due to the phenolic protons of salicylaldimine in case of H_2saldp and was found to be absent in case of its metal complexes implying their formation. It may be noted that the chemical shifts of the complexes are almost similar to those of the free ligand. However, in case of complexes an additional triplet was observed corresponding to the flanked methyl groups at δ = 0.8. For butyl analogs, three set of multiplets at δ = 1.5, 1.31 and 1.29 ppm were observed. Moreover, disappearance of the signal due to O–H proton of the salicylaldehyde is evidenced by the formation of Sn–O bond.

The ^{13}CNMR spectra of the ligand, H_2saldp exhibit signals at δ = 165, 124.5 and 137 ppm corresponding to C_1/C_5, C_2/C_4 and C_3 respectively [39] (Figure 1). These signals are shifted to lower regions in the complexes implying coordination [40] (Table 5). Another set of signals were observed in the region δ = 17.2 and 157 attributed to C_7/C_{16} and C_6/C_{15}. The peaks due to aromatic carbons were observed in the region δ = 112.3–147. However, the C_8/C_{17} were located at δ 167 ppm (Table 5). The methyl carbon attached to tin were observed at about δ = 8.12 ppm [41] while the butyl carbons were observed at about δ = 27.5, 25.4, 25.1 and 13 ppm respectively [42].

Table 5. ^{13}CNMR spectra of the ligand and its complexes

Complex	C_1/C_5	C_2/C_4	C_3	C_6/C_{15}	C_7/C_{16}	C_8/C_{17}
H_2saldp	165	124.5	137	157	17.2	167
Sn(saldp)Me_2	164.5	124.8	137	154	16.4	164
Sn(saldp)Bu_2	164.3	124.3	139	156	15.9	163
Sn(saldp)Me_2MnCl_2	162.9	123.5	136.8	155.2	15.5	161.8
Sn(saldp)Me_2FeCl_2	162.7	122.8	136.7	154.9	15.6	161.8
Sn(saldp)Me_2CoCl_2	163.5	123.9	135.9	155.3	15.7	162.8
Sn(saldp)Me_2NiCl_2	163.9	124.5	138	155.7	15.9	162.1
Sn(saldp)Me_2CuCl_2	162.7	123.5	138.1	155.2	15.7	161.4
Sn(saldp)Bu_2MnCl_2	163.9	124.5	136.8	154.8	15.5	162
Sn(saldp)Bu_2FeCl_2	162.9	123.5	136.8	155.2	15.5	161.9
Sn(saldp)Bu_2CoCl_2	162.7	123.5	138.1	155.7	15.9	162.1
Sn(saldp)Bu_2NiCl_2	162.7	122.8	136.7	154.9	15.6	161.8
Sn(saldp)Bu_2CuCl_2	162.5	123.9	136.8	156	16.1	163.1

Note: ^{13}CNMR of aromatic carbons appear in the region $\delta = 112.3$–147 ppm.

Conclusions

The present work describes the synthesis of heterobimetallic complexes incorporating both transition as well as a non-transition metal ion in close proximity. These complexes may serve as models to mimic polymetallic active sites in biological systems. The methodology employed is high yielding, and analytically pure compounds are obtained.

Acknowledgements

One of the authors (SK) thank the CSIR, New Delhi for financial assistance through grant no. 01(1783)/02/EMR-I and the Department of Chemistry for providing Junior Research Fellowship to SAAN.

References

1. P. Guerriero, S. Tamburini, and P.A. Vigato: *Coord. Chem. Rev.* **110**, 17 (1995).
2. S. Aoki and E. Kimura: *J. Am. Chem. Soc.* **122**, 4542 (2000).
3. N.M. Murthy, M. Mahroof-Tahir, and K.D. Karlin: *Inorg. Chem.* **40**, 628 (2001).
4. J.D. Lee: Concise Inorganic Chemistry, 5th edn., Blackwell Science Ltd., London (2002).
5. F. Meyer and P. Rutsch: *Chem. Commun.*, 1037 (1998); A.M. Barrios and S.J. Lippard: *J. Am. Chem. Soc.* **122**, 9172 (2000); A.M. Barrios and S.J. Lippard: *Inorg. Chem.* **40**, 1250 (2001).
6. J. Glerup, P.A. Goodson, D.J. Hodgson, M.A. Masood, and K. Michelsen: *Inorg. Chim. Acta* **358**, 295 (2005).
7. O. Castillo, I. Muga, A. Luque, J.M. Gutierrez-Zorrilla, J. Sertucha, P. Vitoria, and P. Roman: *Polyhedron* **18**, 1235 (1999).
8. J. Tang, Q. Wang, S. Si, D. Liao, Z. Jiang, S. Yan, and P. Cheng: *Inorg. Chim. Acta* **358**, 325 (2005).
9. K.S. Siddiqi, H. Afaq, S.A.A. Nami, and A. Umar: *Synth. React. Inorg. Met.-Org. Chem.* **33**, 1459 (2003).
10. F. Rafat, K. Siddiqi, and S. Lutfullah: *Synth. React. Inorg. Met. Org. Chem.* **34**, 763 (2004).
11. M. Gilen: *J. Braz. Chem. Soc.* **14**, 870 (2003); S.A. Patil and V.H. Kulkarni: *Polyhedron* **3**, 21 (1984).
12. L.F. Lindoy: *The Chemistry of Macrocyclic Ligand Complexes*, Cambridge University Press, Cambridge (1989).
13. J. Mendham, R.C. Denney, J.D. Barnes, and M. Thomas: *Vogel's Text Book of Quantitative Chemical Analysis*, Pearson Education Asia, Singapore (2002).
14. C.N. Reilly, R.W. Schmid, and F.S. Sadek: *J. Chem. Edu.* **36**, 619 (1959).
15. W.J. Geary: *Coord. Chem. Rev.* **7**, 81 (1971).
16. M. Sonmez: *Synth. React. Inorg. Met.-Org. Chem.* **34**, 733 (2004).
17. M.J. Maroney and N.H. Rose: *Inorg. Chem.* **23**, 2252 (1984).
18. C.T. Aitken and M. Onyszchuk: *J. Organomet. Chem.* **295**, 149 (1985).
19. L. Ronconi, C. Marzano, U. Russo, S. Sitran, R. Graziani, and D. Fergona: *Appl. Organomet. Chem.* **17**, 9 (2003).
20. R.J.H. Clark, P.C. Turtle, D.P. Strommen, B. Streusend, J. Kincaid, and K. Nakamoto: *Inorg. Chem.* **16**, 84 (1977).
21. D. Honnick and J.J. Zuckerman: *Inorg. Chem.* **18**, 1437 (1979).
22. F.A. Cotton, G. Wilkinson, C.A. Murillo, and M. Bochmann: *Advanced Inorganic Chemistry*, 6th edn., Wiley–Interscience, New York (1999).
23. R.N. Prasad and N. Gupta: *J. Serb. Chem. Soc.* **68**, 455 (2003).
24. E. Earnshaw, E.A. King, and L.F. Larkworthy: *J. Chem. Soc. A*, 1048 (1968).
25. F. Calderazzo, F. Floriani, R. Henzi, and F. L'Eplattenier: *J. Chem. Soc. A*, 1378 (1969).
26. H. Furutachi, A. Ishida, H. Miyasaka, N. Fukita, M. Ohba, H. Okawa, and M. Koikawa: *J. Chem. Soc. Dalton Trans.*, 367 (1999).
27. K. Wang, J. Yu, Y. Song, and R. Xu: *J. Chem. Soc. Dalton Trans.*, 99–103 (2003).
28. R.J.M.K. Gebbink, R.T. Jonas, C.R. Goldsmith, and T.D.P. Stack: *Inorg. Chem.* **41**, 4633 (2002).
29. G. Das, R. Shukla, S. Mandal, R. Singh, P.K. Bharadwaj, J.V. Hall, and K.H. Whitmire: *Inorg. Chem.* **36**, 323 (1997).
30. B.J. Hathaway and D.E. Billing: *Coord. Chem. Rev.* **5**, 143 (1970).
31. N.S. Hush and R.J.M. Hobbs: *Prog. Inorg. Chem.* **10**, 259 (1968).
32. M. Julve, M. Verdaguer, M.-F. Charlot, O. Kahn, and R. Claude: *Inorg. Chim. Acta* **82**, 5 (1984).
33. G. Wilkinson, R.D. Gillard, and J.A. McCleverty: *Comprehensive Coordination Chemistry*, Vol. 5, Pergamon Press, Great Britain (1987).
34. J. Rogan and D. Poleti: *Thermochim. Acta* **413**, 227 (2004).
35. L.S. Prabhumirashi and J.K. Khoje: *Indian J. Chem.* **43A**, 299 (2004).
36. L.S. Prabhumirashi and J.K. Khoje: *Thermochim. Acta* **383**, 109 (2002).
37. N.C. Saha, R.J. Butcher, S. Chaudhuri, and N. Saha: *Polyhedron* **22**, 375 (2003).
38. D.M. Boghaei, S.J.S. Sabounchei, and S. Rayati: *Synth. React. Inorg. Met.-Org. Chem.* **30**, 1535 (2000).
39. N.C. Kasuga, K. Sekino, M. Ishikawa, A. Honda, M. Yokoyama, S. Nakano, N. Shimada, N. Shimada, C. Koumo, and K. Nomiya: *J. Inorg. Biochem.* **96**, 298 (2003).
40. L. Mishra, K. Bindu, and S. Bhattacharya: *Indian J. Chem.* **43A**, 315 (2004).
41. H.C. Lim and S.W. Ng: *Acta Crystallograph. Sect. C* **54**, 939 (1998).
42. R. Zhang, J. Sun, and C. Ma: *Inorg. Chim. Acta* **357**, 4322 (2004).